Available online at www.sciencedirect.com

SciVerse ScienceDirect

Advances in Space Research 51 (2013) 492–500

ADVANCES IN SPACE RESEARCH (a COSPAR publication)

www.elsevier.com/locate/asr

Water surface temperature estimation from Landsat 7 ETM+ thermal infrared data using the generalized single-channel method: Case study of Embalse del Río Tercero (Córdoba, Argentina)

Anabel Alejandra Lamaro [a,*], Alejandro Mariñelarena [b,c], Sandra Edith Torrusio [d,e], Silvia Estela Sala [a]

[a] Departamento Científico Ficología, Facultad de Ciencias Naturales y Museo, Universidad Nacional de la Plata, Paseo del Bosque s/n (1900), La Plata, Argentina

[b] Comisión Investigaciones Científicas, Provincia de Buenos Aires, Argentina

[c] Instituto de Limnología "R. Ringuelet", Universidad Nacional de la Plata, CONICET, Argentina

[d] Facultad de Ciencias Naturales y Museo, Universidad Nacional de la Plata, Argentina

[e] Comisión Nacional de Actividades Espaciales, Argentina

Received 2 August 2011; received in revised form 16 July 2012; accepted 22 September 2012
Available online 29 September 2012

Abstract

Monitoring of warm distribution in water is fundamental to understand the performance and functioning of reservoirs and lakes. Surface water temperature is a key parameter in the physics of aquatic systems processes since it is closely related to the energy fluxes through the water–atmosphere interface. Remote sensing applied to water quality studies in inland waterbodies is a powerful tool that can provide additional information difficult to achieve by other means. The combination of good real-time coverage, spatial resolution and free availability of data makes Landsat system a proper alternative. Many papers have developed algorithms to retrieve surface temperature (principally, land surface temperature) from at-sensor and surface emissivity data. The aim of this study is to apply the single-channel generalized method (SCGM) developed by Jiménez-Muñoz and Sobrino (2003) for the estimation of water surface temperature from Landsat 7 ETM+ thermal bands. We consider a constant water emissivity value (0.9885) and we compare the results with radiative transfer classic method (RTM).

We choose Embalse del Río Tercero (Córdoba, Argentina) as case study because it is a reservoir affected by the outlet of the cooling system of a nuclear power plant, whose thermal plume could influence the biota's distribution and biodiversity. These characteristics and the existence of long term studies make it an adequate place to test the methodology.

Values of estimated and observed water surface temperatures obtained by the two compared methods were correlated applying a simple regression model. Correlation coefficients were significant (R^2: 0.9498 for SCGM method and R^2: 0.9584 for RTM method) while their standard errors were acceptable in both cases (SCGM method: RMS = 1.2250 and RTM method: RMS = 1.0426). Nevertheless, SCGM could estimate rather small differences in temperature between sites consistently with the results obtained in field measurements. Besides, it has the advantage that it only uses values of atmospheric water vapor and it can be applied to different thermal sensors using the same equation and coefficients.

Keywords: Water surface temperature; Reservoir; Cooling system; Nuclear power plant; Single-channel generalized method; Atmospheric water vapor

1. Introduction

Reservoirs are built for different purposes like drinking water supply, flood control, irrigation, or power generation

* Corresponding author. Tel.: +54 221 425 7744; fax: +54 221 425 7527.
E-mail address: analamaro@fcnym.unlp.edu.ar (A.A. Lamaro).

0273-1177/$36.00 © 2012 COSPAR. Published by Elsevier Ltd. All rights reserved.
http://dx.doi.org/10.1016/j.asr.2012.09.032

(Casamitjana et al., 2003). Water temperature governs most of the chemical and biochemical processes in aquatic ecosystems. Monitoring of warm distribution in water is fundamental to understand the performance and functioning of reservoirs and lakes (Kimmel et al., 1990), its survey also is important for water quality management, land-use, and hydrological studies (Kay et al., 2005). Surface water temperature is a key parameter in the physics of aquatic systems processes since it is closely related to the energy fluxes through the water-atmosphere interface.

Water temperature surveys using conventional limnological sampling are expensive and time-consuming. Remote sensing applied to water quality studies in inland waterbodies is a powerful tool that can provide systematic and periodic coverage and also additional information from the non-visible regions of the spectrum difficult to achieve by other means (Dash et al., 2002; Novo et al., 2006; Alcântara et al., 2009). Moreover, satellite information allows to obtain data in digital format that can be easily combined with other geographic information, used to generate quantitative models (Chuvieco, 2002) and makes the reduction of field sampling frequency and costs possible. The success of water quality parameters quantification in inland environments depends on water characteristics and the used sensor. The combination of good real-time coverage, spatial resolution and free availability of data makes Landsat system appropriate to study this kind of waterbodies.

During late 20th century, rapid technological advances resulted in increased availability of thermal infrared images and methodologies to calibrate and interpret them. Studies were performed using these data for mapping water surface temperature, especially in places with marked variations – e.g. cooling channels of nuclear power plants, hot springs, etc. (Gibbons and Wukelic, 1989; Mustard et al., 1999; Cherkauer et al., 2005; Zoran et al., 2005; Ahn et al., 2006; Alcântara et al., 2010).

All the energy exchanges between water mass and atmosphere take place within the very thin surface skin layer that can be remotely sensed. Temperature in this layer is typically cooler than the bulk water temperature, so a critical factor to consider is the relationship between these temperatures. Evaporative cooling, wind speed and diurnal energy fluxes affect this complex relationship, nevertheless Yokoyama et al. (1995) and Schneider and Mauser (1996) demonstrated that remotely measured skin temperatures are representative of bulk water temperatures.

Emitted thermal infrared radiation (TIR, $\lambda = 8$–14 μm) can be used to measure temperature of the water surface layer of approximately 100 μm (Kishino et al., 2000; Donlon et al., 2002; Kumar et al., 2003; Kay et al., 2005; Becker and Daw, 2005). After removal of atmospheric and emissivity effects, recovered temperatures should be similar for all TIR sensor bands. The main cause of temperature differences between bands is due to an atmospheric correction problems (typically, atmospheric correction is better at bands around 10–11 μm and worse for bands around 12 μm.) Also, there are other secondary causes mentioned by Kay et al. (2005), such as sensor calibration problems, instrument noise, and in-scene spectral variability from non water materials.

Many papers have developed algorithms to retrieve surface temperature (principally, land surface temperature) from at-sensor and surface emissivity data. In the case of Landsat platform, with one thermal band, the only method that can be applied is a single channel one. Traditionally, the main disadvantages of this kind of method are that some atmospheric parameters are needed for the estimation and they cannot be used for other thermal sensor (Jiménez-Muñoz and Sobrino, 2003).

Jiménez-Muñoz and Sobrino (2003) have developed a generalized single-channel method for retrieving land surface temperature from remote sensing data, called here as: SCGM. This algorithm, assuming that emissivity is known, only uses the total atmospheric water vapor content, the effective wavelength of the sensor and the at-sensor data (brightness temperature or at-sensor radiance). We have applied the SCGM to water surfaces, where emissivity can be considered constant and we used a value of 0.9885 for water emissivity, as calculated by Snyder et al. (1998).

Embalse del Río Tercero is a reservoir affected by the outlet of the cooling system of a nuclear power plant, whose thermal plume could influence the biota's distribution and biodiversity (Mariazzi et al., 1981, 1989; Mariñelarena et al., 1996). These characteristics and long term studies make it an adequate water body to test the methodology.

The aim of this study is to apply the mentioned method for the estimation of water surface temperature of a reservoir using Landsat 7 ETM+ thermal bands.

2. Materials and methods

2.1. Study area

Embalse del Río Tercero (ERT) (32°11′S, 64°25′W) is a medium size reservoir (5400 hm^3, 46 km^2, 45 m max. depth, 12 m mean depth, 0.44 y mean residence time), located in the center of Argentina, in the province of Córdoba (Fig. 1). The reservoir was built in 1936 for flood control, irrigation and hydroelectric purposes. Since 1983 water level fluctuations have been regulated by requirement of a nuclear power plant of 600 MW, which uses its water for cooling purposes. The water inflow to the nuclear plant is located at 15 m deep in the Garganta area (G). Water temperature rises up 7 °C in the cooling system and the outflow is directed through an open cooling channel of 6 km to the southern sector of the reservoir and discharges in a tributary, the Quillinzo River (Mariazzi et al., 1992).

As part of a monitoring program, since 1996 several physical, chemical and biological properties of the ERT waters have been surveyed bimonthly (Mariñelarena et al., annual reports). Surface water temperature is

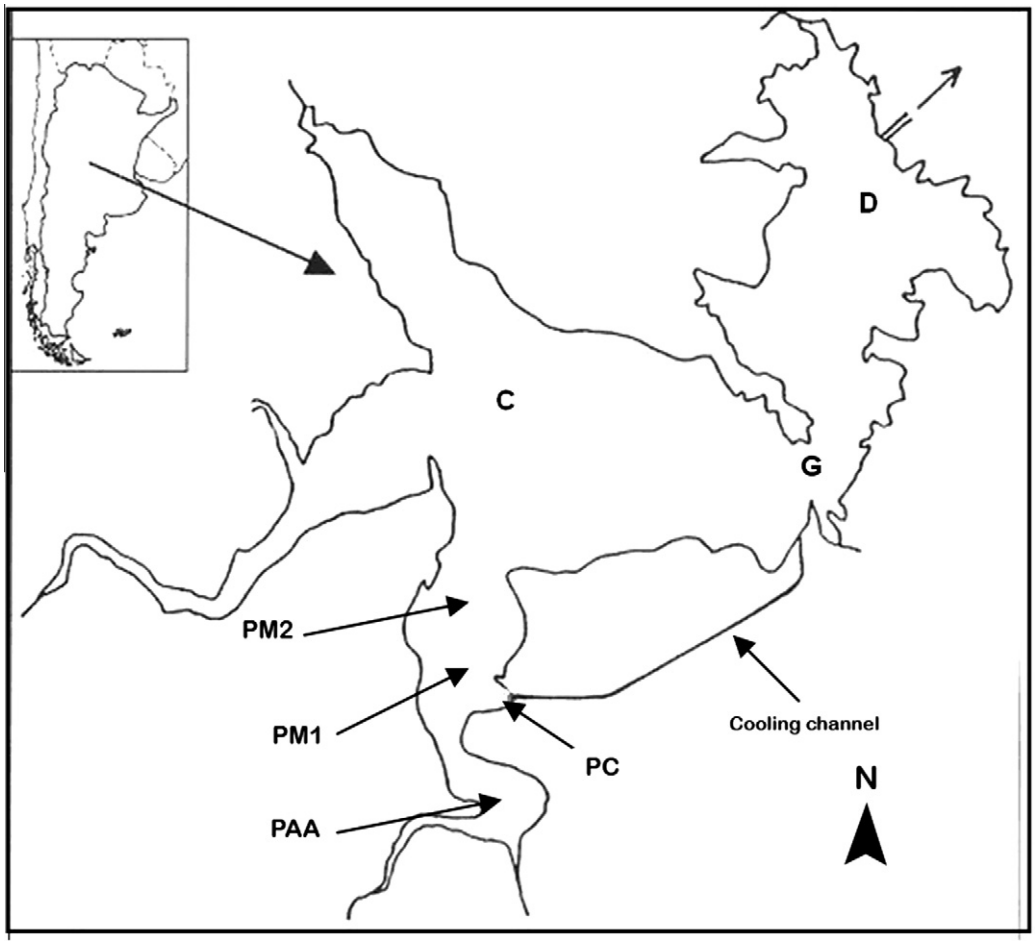

Fig. 1. Location of the sampling stations in Río Tercero Reservoir. References: D: Dique, G: Garganta, C: Confluencia, PM1: Pluma M1, PM2: Pluma M2, PC: Pluma Canal, PAA: Pluma Aguas Arriba.

measured at stations PAA, PC, M1, M2, C, G and D. Results have shown that warmer water released at Quillinzo River forms a thermal plume most of the time restricted to the river channel.

According to these reports, temperature in station G is always lower than that of stations PM1 and PM2. The differences between stations PM1 and G are 3–8 °C (average 4.3 °C, $n = 74$), while between stations PM2 and G differences are 0.5–5 °C (average 2.4 °C, $n = 74$) Mariñelarena (pers. comm.). Nevertheless, in a few dates in 15 years, the temperature of PM2 was lower than that of station G, due to programmed nuclear plant shutdowns and the effect of low temperature of Quillinzo River waters.

2.2. Landsat imagery and processing

In this work we have used images from Landsat 7 ETM+ (Path/Row: 229/82). This sensor has a unique thermal band (band 6) divided into two: low gain band (B6L) and high gain band (B6H), with a spectral resolution from 10.4 to 12.5 μm and a spatial resolution of 60 m covering a surface of 3.600 m^2 per pixel (0.36 ha). Images were obtained from the website of the United States Geological Survey (USGS) (http://glovis.usgs.gov/) and from CONAE. They were in the UTM cartographic projection system, with WGS84 as ellipsoid and datum. They were resampled to 30 m of spatial resolution.

The criteria for the selection of images were:

(1) Existing *in situ* data in ±3 days to the satellite passes.
(2) Images from different seasons in order to find temperature differences.
(3) 0% cloud cover when possible.
(4) No heavy rainfall prior to the image date to minimize the effects of changes in water surfaces that disturb the estimates.

Selected images were: March 19th, 2000; August 13th, 2001; August 16th, 2002; July 10th, 2006 and November 15th, 2006. Software ENVI 4.3 (Research Systems, Inc.) was used for digital processing of images and application of algorithm.

Definition of the specific shoreline for each image is critical to eliminate areas that are not representative of open waters and give inaccurate values of temperatures near the coast (Wang et al., 2008). In order to select pure water

pixels, an unsupervised classification of near-infrared band (Band 4) was made. These classes were used as a mask for obtaining the desired image, thus eliminating the areas of land.

Radiometric conversion of digital numbers (DN) to physical variables (radiance, reflectance and temperature) is very useful in the interpretation of images and to compare data from the same sensor over time or between sensors (Chuvieco, 2002). Digital processing for this conversion involves two main steps: radiometric calibration (Wukelic et al., 1989) and atmospheric correction (Cooper and Asrar, 1989). DN values were converted to at-sensor radiance by applying the gain and bias coefficients of the detectors (Irish, 2006):

$$L_\lambda = gain * DN + bias \quad (1)$$

where L_λ is the uncorrected spectral radiance at λ wavelength in $W * m^2 * sr * \mu m$, DN the digital number, and gain and bias the calibration parameters of detectors (see Table 1).

For the calculation of at-sensor radiative temperature (T_{sat}), radiance values calculated in Eq. (1) were converted to at-sensor radiative temperature using the following equation based on Planck's law (Wukelic et al., 1989):

$$T_{sat} = \frac{K_2}{ln(\frac{K_1}{L_\lambda} + 1)} \quad (2)$$

where T_{sat} is at-sensor radiative temperature (K), K_2 and K_1 = ETM+ thermal constants, $K_2 = 666.09\ W * m^2 * sr * \mu m$ and $K_1 = 1282.71$ K (Chander et al., 2009), and L_λ is the uncorrected spectral radiance at λ wavelength in $W * m^2 * sr * \mu m$.

Generation of water surface temperature images: Landsat 7 ETM+ thermal band 6 Low Gain was used for estimation of water surface temperature. We choose this band because its range is greater and is not saturated (Suga et al., 2003; Weng et al., 2004, Chander et al., 2009). Temperature values estimated for each image were extracted by interpolating the location of the sampling sites using gvSIG free software.

2.3. Methods for water surface temperature estimation

2.3.1. Single Channel Generalized Method (SCGM) (Jiménez-Muñoz and Sobrino, 2003):

SCGM retrieves surface temperature (T_s) using the following general equation:

$$T_s = \gamma[\varepsilon^{-1}(\psi_1 L_\lambda + \psi_2) + \psi_3] + \delta \quad (3)$$

where Γ and δ are parameters dependent on the Planck's function. See Eqs. (7) and (8), ε is the water emissivity. This parameter was considered to be 0.9885 according to Sydner et al. (1998), and L_λ is the uncorrected spectral radiance calculated in Eq. (1), and $\psi 1$, $\psi 2$,$\psi 3$ are the atmospheric functions were calculated by a simulation procedure with MODTRAN 3.5 (Jiménez-Muñoz and Sobrino, 2003). From these values it is easy to obtain the atmospheric functions for every wavelength and for every atmospheric water vapor content (Jiménez-Muñoz and Sobrino, 2003).The values of these functions were calculated by:

$$\psi 1 = 0.14714W^2 - 0.15583W + 1.12340 \quad (4)$$

$$\psi 2 = -1.1836W^2 - 0.37607W - 0.52894 \quad (5)$$

$$\psi 3 = -0.04554W^2 + 1.8719W - 0.39071 \quad (6)$$

where w is the atmospheric water content obtained from http://weather.uwyo.edu/upperair/sounding.html, including date, hour and geographic location (used values of atmospheric water content are shown in Table 2).γ was calculated from:

$$\gamma = \left\{ \frac{C_2 L_\lambda}{T_{sat}^2} \left[\frac{\lambda_{ef}^4}{C_1} L_\lambda + \lambda_{ef}^{-1} \right] \right\}^{-1} \quad (7)$$

where $C_2 = 14387.7\ \mu m\ K$, $C_1 = 1.19104 * 10^8\ W\ \mu m^4$, λ_{ef} = effective wavelength (11.45 μm), L_λ = uncorrected spectral radiance calculated in Eq. (1), T_{sat} is at-sensor radiative temperature (K) calculated in Eq. (2).

δ was calculated from:

$$\delta = -\gamma L_\lambda + T_{sat} \quad (8)$$

where L_λ = uncorrected spectral radiance calculated in Eq. (1). T_{sat} is at-sensor radiative temperature (K) calculated in Eq. (2).

2.3.2. Radiative Transfer Method (RTM)

The atmospheric correction of the radiance of thermal band involves the removal of atmospheric effects that contribute to the signal received by the sensors (up to 90% for

Table 2
Atmospheric water content. Source: http://weather.uwyo.edu/upperair/sounding.html Station identifier: N° 87344. SACO Córdoba Aero Observations (lat.: −31.32 S, long.: −64.22 W).

Landsat scene data	Atmospheric water content (mm)
March 19th, 2000	18.53
August 13rd, 2001	12.50
August 16th, 2002	15.14
July 10th, 2006	13.58
November 15th, 2006	23.33

Table 1
Gains and Biases of Landsat 7 ETM+ thermal bands.

Satellite/sensor	Band	Gain/($W/m^2*sr*\mu m$)/DN	Bias $W/m^2*sr*\mu m$	Source
Landsat 7 ETM+	6 Low gain[a]	0.067087	−0.07	Chander et al. (2009)
	6 High gain	0.037205	3.16	

water), these effects change surface water temperature values of ±2 °C (Kay et al., 2005) considering a constant water emissivity.The uncorrected spectral radiance (L_λ) calculated in Eq. (1) must be correcting taking into account three parts; namely, radiance by surface, reflected downward radiance from atmosphere and upward radiance from atmosphere (Barsi et al., 2003b). The equation used for this correction was (Srivastava et al., 2009):

$$L_{\lambda(T_s)} = \frac{L_\lambda - L_{\lambda up}}{t \bullet \varepsilon_\lambda} - \frac{1-\varepsilon_\lambda}{\varepsilon_\lambda} \bullet L_{\lambda down} \quad (9)$$

where $L_\lambda(T_s)$ is the corrected water surface radiance, L_λ is the uncorrected spectral radiance calculated in Eq. (1), $L_{\lambda up}$ is the upwelling radiance, t is the atmospheric transmissivity, ε_λ is the water emissivity, $L_{\lambda down}$ is the downwelling radiance. Atmospheric parameters ($L_{\lambda up}$, t and $L_{\lambda down}$) were obtained from Atmospheric Correction Parameter Calculator (http://www.atmcorr.gsfc.nasa.gov/) which uses MODTRAN simulator (Barsi et al., 2003).Corrected water surface radiances ($L_\lambda(T_s)$) were subsequently converted into water surface temperature using Eq. (2), which may now be written as:

$$T_s = \frac{K_2}{ln(\frac{k_1}{L_\lambda(T_s)+1})} \quad (10)$$

2.4. Statistical data analysis

From 35 potential points (seven sampling stations and five images), only 27 could be included in the analysis for different reasons (lacking of field data, cloud pixel in the images or land-water mixed pixels). At first instance, all points were analyzed together (observed and estimated water surface temperature). Simple regression analysis was made to evaluate the correlation of estimated water surface temperature obtained by SCGM with *in situ* data. In order to validate the results obtained by the SCGM, the same analysis was performed using the classic method RTM. In addition, for the determination of significant differences between estimated and observed temperature values, Chi square statistic test was applied.

3. Results and discussion

Values of estimated and observed water surface temperatures obtained by the two compared methods were correlated applying a simple regression model. Correlation coefficients were significant (R^2: 0.9426 for SCGM method and R^2: 0.9584 for RTM method) while their standard errors were acceptable in both cases (SCGM method: RMS = 1.2250 and RTM method: RMS = 1.0426). Both models showed very good adjustment, although the RTM fits slightly better (Table 3, Fig. 2A and B). Chi square analysis performed to test these results showed that estimations were accurate (Table 4). Fig. 3 shows data in a time sequence, this type of graph allows us to highlight the accuracy of SCGM. The temperature values estimated by SCGM were higher than those for the RTM (Fig. 3A, B, C and E), but following the same trend that matches the behavior of *in situ* values. Both methods have overestimated observed values, except data of July 2006, when field measurements were underestimated. This situation occurs because in winter there is a greater difference in the temperature between the colder air layer just above the water and the most superficial water layer. As a consequence both methods lost accuracy; however, the trend curves continue being coherent. In August 2002, SCGM overestimated *in situ* data in two of the three sampling stations. At sites D, G, C and PM2, the differences were minor while in

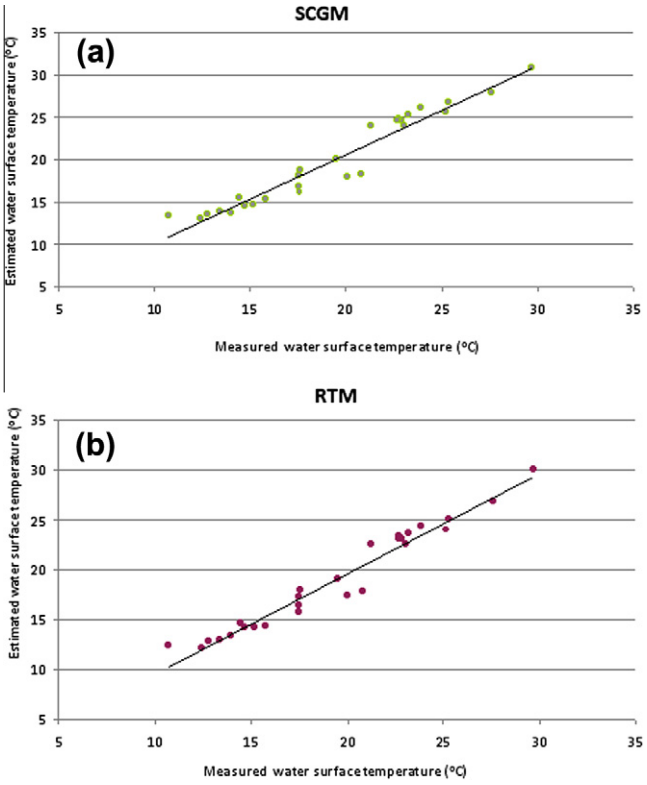

Fig. 2. Plot of estimated water surface temperature versus measured water surface temperature. (a) Single Channel Method (SCGM). (b) Radiative Transfer Method (RTM).

Table 3
Regression statistics of comparison between measured and estimated water surface temperature from both methods.

Methods	Multiple R^2	Adjusted R^2	Standard error of estimate	F	$P(x)$	n
SCGM	0.949855	0.940262	1.224921013	410.2304	0	27
RTM	0.958384	0.956719	1.042623618	575.7314	0	27

Table 4
Chi square test for comparison between measured and estimated water surface temperature from both methods. Critical value: $p < 0.05$ 38.885.

Methods	Chi square	Degree of freedom	$P(x)$
SCGM	2.869466	26	<1
RTM	1.883663	26	<1

the remaining sites (PAA, PC and PM1) differences were higher (up to 3 °C).

Differences in surface water temperature estimated in stations close to the cooling channel (PM1 and PM2) and far from the cooling channel (G) are in agreement with the conclusions of Mariñelarena et al. (annual reports). In all cases the estimated temperatures at station PM1 were higher than those at PM2 and these were higher than those at station G, following a dissipation line from the cooling channel outlet to the lake (Fig. 3).

We built the water surface temperature maps based on SCGM (Fig. 4) considering the obtained results and that

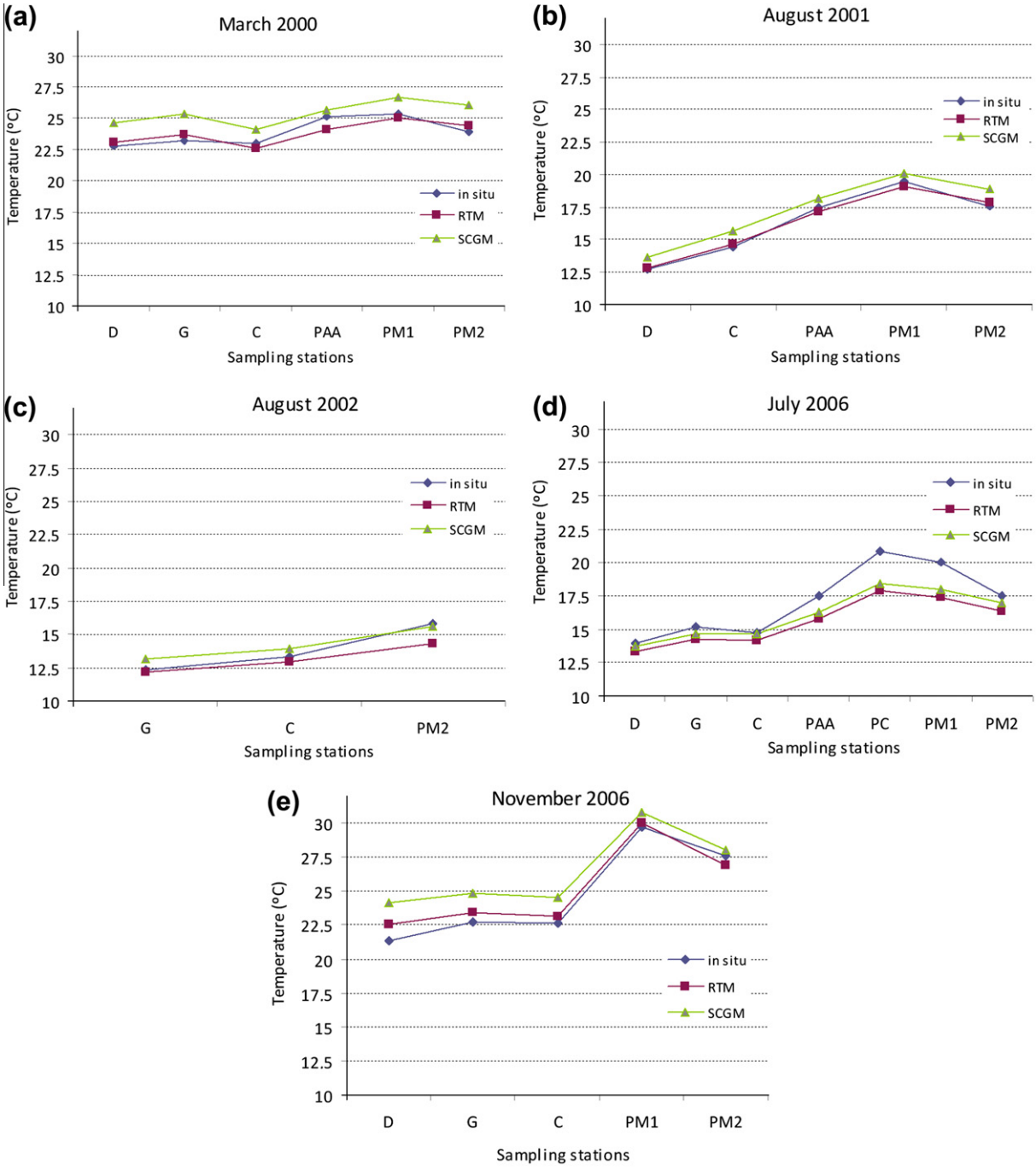

Fig. 3. Comparison of measured and estimated water surface temperature with RTM and SCGM over sampling stations: (a) March 19th, 2000, (b) August 13th, 2001, (c) August 16th, 2002, (d) July 10th, 2006 and (e) November 15th, 2006.

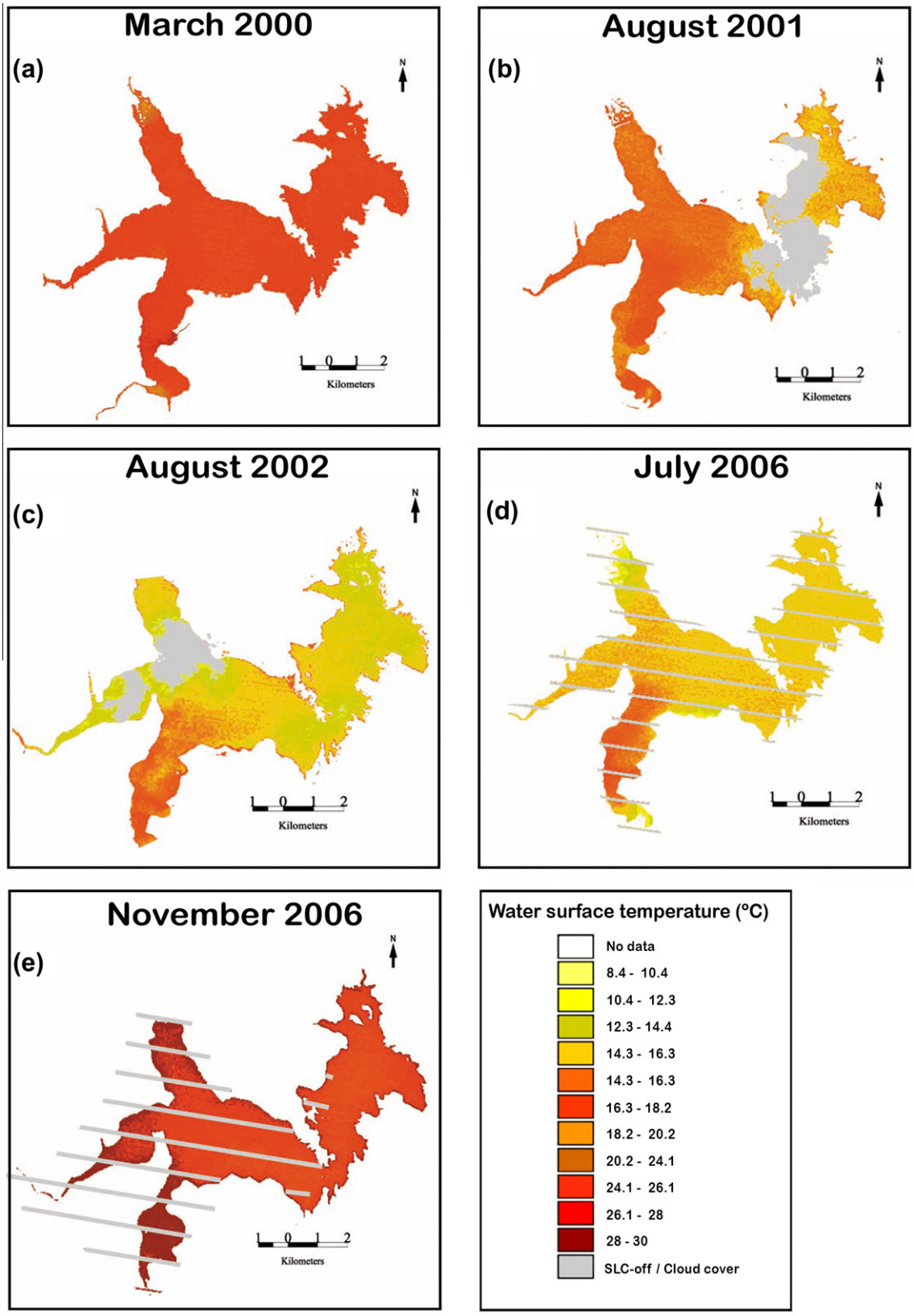

Fig. 4. Water surface temperature maps (°C). (a) March 19th, 2000, (b) August 13th, 2001, (c) August 16th, 2002, (d) July 10th, 2006 and (e) November 15th, 2006.

SCGM uses simple atmospheric data for correction and makes possible its application to different thermal sensors.

It is important to mention that the Single Channel Method was reviewed in 2009. In this review (Jiménez-Muñoz

et al., 2009) they have updated the coefficients involved in the relationship between atmospheric functions ($\psi1$, $\psi2$ and $\psi3$) and atmospheric water vapor (w) for data from the Landsat 5 TM, Landsat 4 and Landsat 7 ETM +. Five different atmospheric sounding databases have been considered to create simulated data used for retrieving atmospheric functions and to test the algorithm. Although in this work we have not applied this review, we compared the obtained RMS values. The comparison with ground-truth data of our values has RMS = 1.2250, which is considered acceptable enough when compared with values obtained by Jiménez-Muñoz et al. (2009). On the other hand, the same authors in 2010 have applied the same algorithm to ASTER satellite data with excellent results (Jiménez-Muñoz and Sobrino, 2010). Our next steps will be directed towards applying this adaptation to our data using images available of the mentioned sensor.

4. Conclusions

Water surface temperature in Embalse del Río Tercero was adequately estimated by both the Single-Channel Method and Radiative Transfer Method. Nevertheless, SCGM could estimate rather small differences in temperature between sites consistently with the results obtained in field measurements. So we conclude that SCGM is the most suitable method to monitor the thermal plume in this reservoir using satellite imagery. Besides, as mentioned above, this method has the advantage that it only uses values of atmospheric water vapor-easily obtained- and it can be applied to different thermal sensors using the same equation and coefficients.

The application of the SCGM developed by Jiménez-Muñoz and Sobrino (2003) provides a simpler tool for the calculation of water surface temperature in this waterbody and expands the possibilities of application in other places with Landsat images or other existing sensors.

References

Ahn, Y., Shanmugam, P., Lee, J., Kang, Y. Application of satellite infrared data for mapping of thermal plume contamination in coastal ecosystem of Korea. Marine Environmental Research 61, 186–201, 2006.

Alcântara, E., Barbosa, C., Stech, J., Novo, E., Shimabukuro, Y. Improving the spectral unmixing algorithm to map water turbidity distributions. Environmental Modelling and Software 24, 1051–1061, 2009.

Alcântara, E., Stech, J., Lorenzzetti, J., Bonnet, M.P., Casamitjana, X., Assireu, A.T., Novo, E. Remote sensing of water surface temperature and heat flux over a tropical hydroelectric reservoir. Remote Sensing of Environment 114 (11), 2651–2665, 2010.

Barsi, J.A., Barker, J.L., Schott, J.R. An Atmospheric Correction Parameter Calculator for a Single Thermal Band Earth-Sensing Instrument. IGARSS03, 21–25 July 2003, Centre de Congres Pierre Baudis, Toulouse, France, 2003a.

Barsi, J.A., Schott, J.R., Palluconi, F.D., Helder, D.L., Hook, S.J., Markham, B.L., Chander, G., O'Donnell, E.M. Landsat TM and ETM+ thermal band calibration. Canadian Journal of Remote Sensing 28, 141–153, 2003b.

Becker, M.W., Daw, A. Influence of lake morphology and clarity on water surface temperature as measured by EOS ASTER. Remote Sensing of Environment 99, 288–294, 2005.

Casamitjana, X., Serra, T., Baserba, C., Pérez-Losada, J. Effects of the water withdrawal on the stratification patterns of a reservoir. Hydrobiologia 504, 21–28, 2003.

Chander, G., Markham, B.L., Helder, D.L. Summary of current radiometric calibration coefficients for Landsat MSS, TM, ETM+, and EO-1 ALI sensors. Remote Sensing of Environment 113, 893–903, 2009.

Cherkauer, K.A., Burges, S.J., Handcock, R.N., Kay, J.E., Kampf, S.K., Gillespie, A.R. Assessing satellite-based and aircraft-based thermal infrared remote sensing for monitoring Pacific Northwest River temperature. Journal of the American Water Resources Association (JAWRA) 41 (5), 1149–1159, 2005.

Chuvieco, E. Teledetección Ambiental (Environmental Remote Sesning). 1st ed. Ariel S.A., Barcelona, Spain. 586 pp., 2002 (in Spanish).

Cooper, D.I., Asrar, G. Evaluating atmospheric correction models for retrieving surface temperatures from the AVHRR over a tall grass prairie. Remote Sensing of Environment 27, 93–102, 1989.

Dash, P., Göttsche, F.M., Olesen, F.S., Fischer, H. Land surface temperature and emissivity estimation from passive sensor data: theory and practice-current trends. International Journal of Remote Sensing 23, 2563–2594, 2002.

Donlon, C.J., Minnett, P., Gentemann, C. Towards improved validation of satellite sea surface skin temperature measurements for climate research. Journal of Climate 15, 353–369, 2002.

Gibbons, D.E., Wukelic, G.E. Application of Landsat thematic mapper data for coastal thermal plume analysis at Diablo Canyon. Photogrammetric Engineering and Remote Sensing 55, 903–909, 1989.

Irish, R.R. Landsat 7 Science Data Users Handbook. National Aeronautics and Space Administration (NASA). Report N° 430–15-01-003-0, 2006.

Jiménez- Muñoz, J.C., Sobrino, J.A. A generalized single-channel method for retrieving land surface temperature from remote sensing data. Journal of Geophysical Research 108 (D22), 2003.

Jiménez-Muñoz, J.C., Cristóbal, J., Sobrino, J.A., Sòria, G., Ninyerola, M., Pons, X. Revision of the single-channel algorithm for land surface temperature retrieval from Landsat thermal-infrared data. IEEE Geoscience and Remote Sensing Letters 47 (1), 2009.

Jiménez- Muñoz, J.C., Sobrino, J.A. A single-channel algorithm for land-surface temperature retrieval from ASTER data. IEEE Geoscience and Remote Sensing Letters 7 (1), 2010.

Kay, J.E., Kampf, S.K., Handcock, R.N., Cherkauer, K.A., Gillespie, A.R., Burges, S.J. Accuracy of lake and stream temperatures estimated from thermal infrared images. Journal of the American Water Resources Association 41, 1161–1175, 2005.

Kimmel, B.L., Lind, O.T., Paulson, L.J. Reservoir primary production, in: Thorton, K.W., Kimmel, B.L., Payne, F.E. (Eds.), Reservoir Limnology. Ecological Perspectives. John Wiley and Sons, New York, 1990.

Kishino, M., Matsunaga, T., Abrams, M., Kato, M. Water quality and temperature mapping using ASTER, in: International Geoscience and Remote Sensing Symposium (IGARSS) 2000, Honolulu, Hawaii, 2000.

Kumar, A., Minnett, P.J., Podestá, G., Evans, R.H. Characteristics of the atmospheric correction algorithms used in retrieval of sea surface temperatures from infrared satellite measurements: global and regional aspects. Journal of the Atmospheric Sciences 60, 575–585, 2003.

Mariazzi, A.A., Romero, M.C., Villalobos, E.R., Di Siervi, M.A., Mariñelarena, A. Estudio bacteriológico en el Embalse del Río III (Provincia de Córdoba, Argentina). Factores ecológicos, predicciones sobre efectos térmicos. Limnobios, 2, 89–110, 1981 (in Spanish).

Mariazzi, A.A., Romero, M.C., Conzonno, V.H., Mariñelarena, A. Results of a limnological study in a reservoir previous to the functioning of a nuclear power plant (Embalse del Rio III). Revista de la Asociación de Ciencias Naturales del Litoral, 20 (1 and 2), 57–68, 1989.

Mariazzi, A.A., Donadelli, J.L., Arenas, P., Di Siervi, M.A., Bonetto, C. Impact of a nuclear power plant on water quality of Embalse del Río

Tercero Reservoir, (Córdoba, Argentina). Hydrobiologia 246, 129–140, 1992.

Mariñelarena, A.J., Casco, M.A., Claps, M.C., Di Siervi, M.A., Donadelli J.L., Hechem, M.A., Mac Donagh, M.E., Ardohain, D.M. Estudio Limnológico del Embalse del Río Tercero, (Córdoba). Annual Reports to Central Nuclear Embalse, 1996 – Present (in Spanish).

Mustard, J.F., Carney, M.A., Sen, A. The use of satellite data to quantify thermal effluent impacts. Estuarine, Coastal and Shelf Science 49, 509–524, 1999.

Novo, E.L., Barbosa, C.C.F., Freitas, R.M., Shimabukuro, Y.E., Melack, J.M., Pereira-Filho, W. Seasonal changes in chlorophyll distribution in Amazon floodplain lakes derived from MODIS images. Limnology 7, 153–161, 2006.

Schneider, K., Mauser, W. Processing and accuracy of Landsat thematic mapper data for lake surface temperature measurement. International Journal of Remote Sensing 17, 2027–2041, 1996.

Snyder, W.C., Wan, Z., Zhang, Y., Feng, Y.Z. Classification-based emissivity for land surface temperature measurement from space. International Journal of Remote Sensing 19 (14), 2753–2774, 1998.

Srivastava, P.K., Majumdar, T.J., Bhattacharya, A.K. Surface temperature estimation in Singhbhum Shear Zone of India using Landsat-7 ETM+ thermal infrared data. Advances in Space Research 43 (10), 1563–1574, 2009.

Suga, Y., Ogawa, H., Ohno, K., Yamada, K. Detection of surface temperature from Landsat 7 ETM+. Advances in Space Research 32 (11), 2235–2240, 2003.

Wang, L.T., McKenna, T.E., De Liberty, T.L. Locating Ground water discharge areas in Rehoboth and Indian river bays and Indian river, Delaware using Landsat 7 imagery. Report of Investigations N° 74. University of Delaware and Delaware Geological Survey: 17, 2008.

Weng, Q., Lu, D., Schubring, J. Estimation of land surface temperature vegetation abundance relationship for urban heat island studies. Remote Sensing of Environment 89, 467–483, 2004 .

Wukelic, G.E., Gibbons, D.E., Martucci, I.M., Foote, H.P. Radiometric calibration of Landsat thematic mapper thermal band. Remote Sensing of Environment 28, 339–347, 1989 .

Yokoyama, R., Tanba, S., Souma, T. Sea surface effects on the sea surface temperature estimation by remote sensing. International Journal of Remote Sensing 16, 227–238, 1995 .

Zoran M.A., Nicola D.N., Talianu, C.L., Ciobanu, M., Ciuciu, J.G. Analyses of thermal plume of Cernavoda nuclear power plant by satellite remote sensing data, in: Manfred Ehlers, Ulrich Michel (Eds.), Proceedings of the Remote Sensing for Environmental Monitoring, GIS Applications, and Geology V, 2005.